Desalination and Water Treatment
www.deswater.com
doi: 10.5004/dwt.2021.26699

214 (2021) 273–285
February

Influence of the procedure of casting solution preparation on the antimicrobial properties of polyethersulfone membranes modified with titanate nanotubes

Sylwia Mozia[a,*], Paulina Sienkiewicz[a], Kacper Szymański[a], Dominika Darowna[a], Adam Czyżewski[a], Michał Zgrzebnicki[b]

[a]*Department of Inorganic Chemical Technology and Environment Engineering, Faculty of Chemical Technology and Engineering, West Pomeranian University of Technology in Szczecin, ul. Pułaskiego 10, 70-322 Szczecin, Poland, Tel. +48 91 449 47 30; email: sylwia.mozia@zut.edu.pl (S. Mozia)*
[b]*Department of Catalytic and Sorbent Materials Engineering, Faculty of Chemical Technology and Engineering, West Pomeranian University of Technology in Szczecin, ul. Pułaskiego 10, 70-322 Szczecin, Poland*

Received 30 April 2020; Accepted 18 May 2020

ABSTRACT

The influence of the titanate nanotubes (TNTs) on the antimicrobial properties of mixed-matrix polyethersulfone membranes obtained by the wet phase inversion is discussed in relation to the procedure of preparation of casting solution. Various attempts to TNTs dispersion in the polymer-solvent (*N,N*-dimethylformamide) were investigated, based on the application of ultrasonic bath (indirect sonication) or ultrasonic probe (direct sonication). The antimicrobial properties of the membranes were evaluated using *Escherichia coli*. The physicochemical properties of the membranes were assessed based on scanning electron microscopy, atomic force microscopy, and isoelectric point measurements. It was found that the direct sonication led to the formation of smaller TNTs agglomerates compared to the indirect method. As a result, the membranes obtained with the application of the former technique exhibited smoother surface and higher water permeability compared to the membranes fabricated with the latter approach. A linear correlation between mean surface roughness (R_a) and inhibition of bacterial growth was proved. The best antimicrobial performance exhibited the membrane characterized by the highest R_a, prepared with the application of the indirect sonication. The inhibition of *E. coli* growth after 24 h of incubation in the presence of this membrane was about five times higher than that observed for the unmodified membrane.

Keywords: Polyethersulfone membrane; Titanate nanotubes; Roughness; Antimicrobial activity; *Escherichia coli*

1. Introduction

Over the past few decades the membrane-based technologies have experienced rapid development and are now being frequently used in various industrial fields and processes, such as desalination, water, and wastewater treatment, or in dairy and pharmaceutical industries [1–7]. However, despite the progress made, the present-day membrane techniques still suffer from the limited resistance of the membranes to the fouling effect. Membrane fouling is characterized by the accumulation of feed components onto the surface of a membrane or within its pores, resulting in a decrease of permeate flux, shortage of the membranes lifespan, and the increase of the energy consumption and overall costs of the membrane filtration processes.

Depending on the type of foulant deposited on the membrane surface, fouling phenomenon can be differentiated into a few categories, such as organic fouling, inorganic fouling (scaling), colloidal fouling, and biological fouling. The latter, also denoted as biofouling, is associated with

* Corresponding author.

the formation of biofilm on the membrane surface, caused by the attachment, accumulation, and growth of microorganisms. In comparison with the other types of fouling, biofouling is considered to be more troublesome, mostly due to the constant growth and rapid multiplication of the microorganisms.

One of the common practices to prevent the formation of biofilm involves the pre-treatment of feed water with biocides or antimicrobial substances. However, some of the biocides, like chlorine or chloramines are known to produce toxic disinfection by-products, such as trihalomethanes, *N*-nitrosodimethylamine, and haloacetic acids, capable of membrane penetration [8]. Furthermore, it was confirmed that biocides can damage the surface structure of polymeric membranes [9]. Another issue is that the biocide treatment is not a fully effective procedure. Namely, it can reduce, even significantly, the amount of microorganisms, but it cannot hinder the re-growth of the residual cells. In addition, it is often stated that biocide treatment can indirectly promote microbial growth, due to the formation of the assimilable organic carbon (AOC) [10,11].

In view of the above limitations of the commonly applied anti-biofouling methods, there is an urgent and constant need for the development of new and more effective fouling mitigation strategies. To that end some researchers have turned their attention to the development of new types of polymeric membranes which exhibit improved performance, not only in terms of anti-biofouling properties, but also permeability and solute rejection. In general, three different approaches were proposed, including chemical treatment, surface grafting, and additive blending. The first two groups of methods can be viewed as more complex and often include many post-treatment processes. In contrast, the additive blending method, not only discludes the need for any additional steps during the membrane preparation, but also allows to introduce the desired additive directly into the casting solution.

In searching for suitable additives many researchers have turned their attention towards different types of nanoparticles (NPs), such as silica (SiO_2), titania (TiO_2), alumina (Al_2O_3), zirconia (ZrO_2), zerovalent iron (ZVI, Fe), carbon nanotubes (CNTs), halloysite nanotubes (HNTs), silver (Au), gold (Ag), and palladium (Pd) [12–19]. However, due to their high intra-aggregate interactions, the nanoparticles blended with a polymer have a tendency to agglomerate. This can lead not only to the uneven distribution of NPs in the polymeric matrix, but can also affect the mechanical strength of the membrane [20]. In addition, it was confirmed that the formation of large agglomerates may also influence the membrane topography due to the formation of hills and valleys on the surface, which can enhance the attachment of bacteria and thus contribute to the biofouling [21].

The recent advances made in the field of nanotechnology have given rise to the formation of new nano-sized species, such as titanate or titania nanotubes (TNTs). It was confirmed that TNTs are characterized not only by their highly hydrophilic properties, but are also known to exhibit a well-developed porous structure and large specific surface area [22,23]. These properties can be utilized for fabrication of membranes with improved antifouling characteristics as well as transport and separation performance. The studies on the utilization of TNTs in membrane preparation are, however, very limited. Abdallah et al. [24] and Sumisha et al. [25] have reported on the preparation of TNTs-modified polymeric membranes with enhanced desalination performance. Other studies [26,27] have shown that the incorporation of TNTs into the polymeric membranes can improve water flux, separation performance, and antifouling properties of the membrane. More recent finding have also proved that the permeability and antifouling properties of the hybrid membranes can be furtherly improved by using functionalized TNTs, pre-treated with sulfuric acid to attain sulfated TNTs or modified with [(2-amino-ethyl)-3-aminopropyl] trimethoxysilane to introduce amine groups on TNTs surface [28,29]. Moreover, Subramaniam et al. [30] have also fabricated novel TNTs-modified hollow fiber polyvinylidene fluoride (PVDF) ultrafiltration membranes utilized for decolorization of aerobically-treated palm oil mill effluent. The same group of authors have confirmed that the PVDF-TNTs membranes can be successfully applied in a submerged membrane photoreactor achieving promising performance in terms of color removal, flux, and low membrane fouling susceptibility [31]. Recently, Raeisi et al. [32] prepared TNTs–incorporated poly(vinyl alcohol) (PVA) mixed matrix membranes dedicated for pervaporation process. The studies revealed that the addition of hydrophilic TNTs might improve the properties of PVA membranes in terms of both permeability and separation factor. The recent works of our group have also confirmed the advantages of the application of Ag-modified TNTs [33] and Cu-modified TNTs [34] for polyethersulfone (PES) membranes fabrication. The mixed-matrix membranes were characterized by increased water permeability as well as improved antifouling and antibacterial performance. However, the literature is lacking in reports regarding the antimicrobial properties of the composite membranes modified with pure TNTs, which are especially important when the biofouling issues are considered.

In the present paper, the influence of the preparation procedure on the antibacterial and separation properties of TNTs-modified PES membranes obtained by the wet phase inversion method is presented and discussed. In order to limit the agglomeration of TNTs in the polymer matrix, several dispersion methods were devised using two types of sonication techniques (direct and indirect). To explain the antimicrobial performance of the membranes their morphology and topography was analyzed in details.

2. Experimental

2.1. Materials

PES polymer (VERADEL® PESU, Solvay, Belgium, provided by Solvay Poland Sp. z o. o.) and *N*,*N*-dimethylformamide (DMF) solvent (Avantor Performance Materials Poland S.A., Poland, puriss p.a.) were used for preparation of membrane casting solution. Commercially available TiO_2 Aeroxide® P25 (Evonik, Germany) was applied as a substrate for TNTs synthesis. HCl (35–38 wt.%, puriss) and NaOH (puriss p.a.) used during the TNTs preparation were purchased from Avantor Performance Materials Poland S.A. (Poland). Polyethylene glycols (PEG, molecular weight

(MW) of 2–35 kDa, Sigma-Aldrich, USA) and dextrans with MW of 70–500 kDa (Polfa Kutno, Poland) were applied for the determination of the separation properties of the prepared membranes. KCl (puriss p.a.), KOH (puriss p.a.), and HCl (36–38 wt.%, puriss p.a.) used during the isoelectric point measurements were purchased from Avantor Performance Materials Poland S.A. (Poland).

The agar plates used in the microbial experiments were prepared using the Plate Count Agar (BIOMAXIMA, Poland). NaCl (Merck, Germany) was employed for preparation of saline solution (8.5 g/L). The *Escherichia coli* bacteria strain K12 (ATCC 29425, USA) was selected as model microorganism. The initial concentration of bacteria suspension applied in the experiments was set at 0.5 according to McFarland scale.

In all experiments pure (type 2) water (Elix 3, Millipore) was used unless otherwise stated.

2.2. Preparation of titanate nanotubes

TNTs were prepared using the hydrothermal method introduced and described by Kasuga et al. [35]. First, 0.5 g of TiO_2 and 60 mL of 10 M NaOH were added to a 75 mL Teflon-lined vessel. The obtained mixture was sonicated in ultrasonic bath for 1 h. The hydrothermal process was carried out for 24 h at 140°C in BLH-800 pressure reactor (Berghof, Germany). The obtained product was washed with 0.1 M HCl solution, followed by pure water rinsing until the conductivity of washing solution (measured using Ultrameter II, Myron L Company, USA) was below 2 μS/cm. The washed nanomaterial was centrifuged at 3,000 rpm for 10 min (Universal 320R, Hettich, Germany). The last step included drying (80°C for 24 h) and grinding of TNTs in an agate mortar.

2.3. Preparation of casting solution

The unmodified PES membrane (15 wt.% of polymer in DMF), denoted as *M*1, was prepared by dissolution of 8.38 g PES in 50 mL of DMF. A tightly sealed glass bottle containing the components was magnetically stirred until the polymer was completely dissolved. After mixing the casting dope was left for degassing and subsequently casted on a glass plate using an automatic film applicator (Elcometer 4340, Elcometer Ltd., UK) with a knife gap set at 0.1 mm. The casted film was immersed in the pure water coagulation bath at 20°C for 24 h.

The TNTs-modified membranes, denoted as *M*2–*M*7, were prepared according to two various procedures (Table 1). The concentration of TNTs in every case remained unchanged, that is, 1 wt.% in relation to PES.

- *Procedure No*. 1: in the first step, 8.38 g of PES was dissolved in 40 mL of DMF (solution *A*). Then, a suspension of TNTs (0.0838 g) in DMF (10 mL) was prepared by sonication in ultrasonic bath (Sonic-6D, Polsonic, Poland; output power 320 W, frequency 40 kHz) (solution *B*). Three sonication durations were investigated: 0.5 h (*M*2), 2.5 h (*M*3), and 5 h (*M*4). Subsequently, solution *B* was added to solution *A* and mixed using magnetic stirrer (200 rpm) for 2 h. Such obtained casting dope was used for membrane preparation according to the same procedure as in the case of *M*1.
- *Procedure No*. 2: in the first step, 8.38 g of PES was dissolved in 40 mL of DMF (solution *A*). Then, a suspension of TNTs (0.0838 g) in DMF (10 mL) was prepared by sonication using ultrasonic liquid processor (Vibra-cell VCX-130, Sonics, USA; output power 130 W, frequency 20 kHz) equipped with a 6 mm ultrasonic probe (solution *C*). Three sonication amplitudes were investigated: 40% (*M*5), 60% (*M*6), and 80% (*M*7). Subsequently, solution *C* was added to solution *A* and mixed using a magnetic stirrer (200 rpm) for 2 h. The membranes were casted according to the same procedure as described earlier.

2.4. Characterization of TNTs and membranes

The phase composition of the nanotubes was evaluated based on X-ray diffraction (XRD) analysis (PANalytical Empyrean X-ray diffractometer) using CuKα radiation (λ = 1.54056 Å). The morphology of TNTs was examined with application of transmission electron microscopy (TEM) FEI Tecnai F20. Before analysis, the sample was dispersed in ethanol by sonication, and the obtained suspension was dropped on a copper grid (300 mesh).

The isoelectric point of the prepared membranes was measured using SurPASS 3 analyzer (AntonPaar, Austria). The solution of 0.001 M KCl in ultrapure water (Simplicity®, Millipore) was used as an electrolyte. The pH was adjusted using HCl and KOH solutions.

The morphology of membranes was evaluated using Hitachi (Japan) SU8020 ultra-high resolution field emission scanning electron microscopy (UHR FE-SEM). Accelerating voltage was 5 kV. Before measurement, the membranes were dried in water–ethanol solutions. In order to examine the cross-sections, the membranes were crushed in liquid nitrogen. The samples were mounted on a table using

Table 1
Summary of the procedures of membranes preparation (*A* – amplitude)

		Unmodified	Procedure No. 1			Procedure No. 2		
		*M*1	*M*2	*M*3	*M*4	*M*5	*M*6	*M*7
Stage 1	Ultrasonic bath	–	0.5 h	2.5 h	5 h	–	–	–
	Ultrasonic probe	–	–	–	–	0.5 h, *A*:40%	0.5 h, *A*:60%	0.5 h, *A*:80%
Stage 2	Magnetic stirring (2 h)	+	+	+	+	+	+	+

carbon tape and coated with a chromium layer by utilizing the Q150T ES coater (Quorum Technologies Ltd., UK).

The topography of the membranes surface was evaluated on a basis of atomic force microscopy (AFM) using NanoScope V multimode 8 scanning probe microscopy (Bruker Corp., USA). The measurements were realized with the silicon nitride ScanAsyst – air probe in the ScanAsyst mode. The scanned area was 10 μm × 10 μm. The mean roughness (R_a) of the membranes surface was evaluated using NanoScope Analysis software.

The transport and separation properties of the membranes were determined using laboratory scale ultrafiltration installation. The system was equipped with a suction pump with a pressure dampener, a stainless steel membrane module (with a 1.194 mm feed spacer), a manometer, and a needle valve. Membrane working (effective) area was 0.0025 m^2. The pure water flux (PWF) was evaluated at the transmembrane pressure (TMP) of 1, 2, and 3 bar and the feed cross-flow velocity (VCF) of 0.5 m/s. The temperature was maintained at 20°C ± 1°C. The changes of the permeate flux were determined by measuring the volume of liquid permeating through the membrane during a fixed period of time. Each experiment was repeated at least 4 times in order to confirm reproducibility of the results.

The separation properties of the membranes were determined at TMP = 2 bar using dextran or PEG solutions (1 g/L). The concentrations of the model compounds in feed (C_f) and permeate (C_p) were measured using high performance liquid chromatography LaChrom Elite (Hitachi, Japan) equipped with the refractive index detector L-2490 and the polySep-GFC-P4000 column. Ultrapure water (simplicity®, Millipore) was used as a mobile phase. The rejection coefficient (R) was calculated according to Eq. (1):

$$R = \frac{C_f - C_p}{C_f} \times 100\% \quad (1)$$

2.5. Microbiological research

2.5.1. Preparation of culture medium

Sterile plastic Petri dishes were filled with liquid Plate Count Agar (PCA), previously prepared in accordance with manufacturer indications. After the agar had solidified, the plates were sterilized under UVC radiation for 20 min and then dried in the incubator at the temperature of 30°C for 3 d.

2.5.2. Bacteria counting

The technique of serial decimal dilutions in saline solution (8.5 g/L NaCl) was applied for bacteria counting. A 0.3 mL aliquot of an appropriate dilution was placed on the agar plate and spread. Three replications for each dilution were performed. The inoculated plates were incubated at the temperature of 37°C for 24 h. Then, the visible *E. coli* colonies on the Petri dishes were counted using the LKB 2002 counter (POL-EKO, Poland). The results were calculated as the average colony-forming unit (CFU) per mL according to Eq. (2):

$$\text{CFU/mL} = \frac{n \times x}{v} \quad (2)$$

where n is the number of bacteria colonies visible on a Petri dish, x is the dilution factor, and v is the volume of bacteria suspension placed on the Petri dish (0.3 mL).

2.5.3. Testing of antimicrobial properties of the membranes

A piece of a dry membrane (12.5 cm × 4.5 cm), previously dehydrated in ethanol, was introduced to a Duran glass bottle containing 100 mL of bacteria suspension in saline solution (optical density of 0.5 according to McFarland scale). After adding an elliptical magnetic stirring bar, the bottle was kept on a magnetic stirrer for 24 h, with the temperature and mixing speed set at 37°C and 250 rpm, respectively. Blank tests were prepared under the same conditions but in the absence of a membrane. All experiments were repeated at least three times. The rate of inhibition of bacterial growth was evaluated on a basis of log reduction and calculated as follows (Eq. (3)):

$$\text{log reduction} = \log\left(\frac{B}{S}\right) \quad (3)$$

where B is the amount of bacteria (CFU/mL) in a blank sample, S is the amount of bacteria (CFU/mL) in the presence of a membrane.

3. Results and discussion

3.1. Characteristics of TNTs

Fig. 1 illustrates the XRD pattern of the as-prepared TNTs. Three major peaks, positioned at 2θ angle of ca. 24.5° (110), 28.5° (211), and 48.5° (020), can be observed. The peaks can be ascribed to the layered titanates such as $H_2Ti_2O_5 \cdot H_2O$, $H_2Ti_3O_7$, and $H_xTi_{2-x/4}\square_{x/4}O_4$ ($x \approx 0.7$, □: vacancy) [36–38].

The morphology of TNTs was analyzed using TEM (Fig. 2). The nanotubes have a cylindrical shape and a uniform diameter across the entire length. The TNTs exhibited an average inner/outer diameter of about 4–8/8–12 nm and length in the range of about 50–150 nm.

3.2. Physicochemical properties and morphology of membranes

Fig. 3 presents SEM cross-sections of the unmodified *M*1 membrane and the composite *M*2–*M*7 membranes. No significant differences in the morphology of the membranes obtained under various procedures can be seen. All the membranes are characterized by an asymmetric structure with a thin skin layer, a sublayer build of narrow finger-like pores, and a bottom layer with large finger-like pores expanding toward the membranes edge, with a spongy structure between them. Moreover, some spherical shape macrovoids can be also observed in the lower parts of the cross-section.

In case of the mixed-matrix membranes some TNTs agglomerates were also found in the SEM images. Fig. 4 presents as an example the agglomerates observed in the cross-sections of *M*2 and *M*4 membranes prepared according to procedure No. 1, and *M*6 and *M*7 membranes fabricated in line with the procedure No. 2. In general, the sizes of the agglomerates in the former case were larger compared to the latter. The largest TNTs agglomerates

(with diameters even up to 13 μm) were observed for *M*2 in case of which the time of treatment in the ultrasonic bath was the shortest (0.5 h). Most of the agglomerates detected in *M*4, prepared with application of TNTs suspension sonicated for 5 h, were smaller, with typical diameters of 3–7 μm, although some larger formations (up to 9 μm) were also noted. The size of TNTs agglomerates observed in the cross-sections of *M*6 and *M*7, fabricated with utilization of the ultrasonic probe, in most samples did not exceed 4 μm. In the case of *M*7, the species of dimensions as low as 1–2 μm were also found. The observed differences in the dispersion of TNTs were attributed to the various efficiency of sonication due to a different way of energy transfer in the case of ultrasonic bath and ultrasonic probe. The sonication in the ultrasonic bath (indirect method) is in general less effective because the energy is being spread diffusively. On the opposite, for the ultrasonic probe (direct method) in which case the energy is focused on a localized sample zone [39], a more efficient cavitation in the liquid is obtained leading to a more efficient reduction of the TNTs agglomerates size.

To further explain the relationship between the applied TNTs dispersion method and the properties of the membranes, the surfaces of the membranes were characterized by means of AFM microscopy (Fig. 5).

The obtained images revealed some differences in the dispersion of TNTs in the polymer matrix, confirming the presence of different-sized agglomerates on/under the surface of the composite membranes. Similarly as shown by SEM analysis, the size of the agglomerates depended on the dispersion method. The largest hills on the membrane surface were observed when the procedure No. 1 with the ultrasonic bath was used. The *M*2 and *M*3 membranes were characterized by the presence of single quite large agglomerates with diameters in the range of 1.4–3.6 and 1.6–4.7 μm, respectively. The elongation of the time of sonication to 5 h resulted in the formation of both round (oval) structures (up to 7.9 μm width) and needle-like pillars significantly protruding above the *M*4 membrane surface (ca. 0.1–0.9 μm width). The height of these structures varied from about 30 nm even up to ca. 550 nm, indicating a very non-uniform topography of the surface. The ultrasonic probe used in procedure No. 2 allowed to improve the dispersion of TNTs on the membranes surface, which was especially visible in the case of *M*6 and *M*7. The agglomerates observed for these membranes were either in the form of wide hills (1.5–3.5 μm width and 75 nm height) or narrow peaks (less than 0.4 μm width and 120 nm height). However, no clear correlation between the size of these species and the sonication amplitude was found. The smaller size of the TNTs formations determined by AFM in comparison to those obtained by SEM analysis can be explained by the partial coverage of the agglomerates with PES and their embedding in the polymer matrix.

On a basis of the AFM analysis the mean surface roughness (R_a) of the membranes was calculated (Fig. 6).

All the mixed-matrix membranes were characterized by more rough surfaces than the unmodified membrane (*M*1). Moreover, the roughness of the membranes prepared according to procedure No. 1 was higher (10.1–16.7 nm) compared to R_a of the membranes fabricated with the application of procedure No. 2 (8.2–9.9 nm). This is in agreement with the results of the SEM analysis discussed above. Better dispersion of TNTs under the action of the ultrasonic probe led to the formation of smaller TNTs aggregates, which presents on the surface of the membranes resulted in only a slight increase of the R_a value. On the opposite, poorer deagglomeration of TNTs in the case of the application of ultrasonic bath resulted in the formation of larger aggregates, which contributed to a higher increase of roughness than observed in the case of the ultrasonic probe. Moreover, the aggregates on the surface of *M*2–*M*4 membranes were more non-uniform than in the case of *M*5–*M*7, as can be found from the standard deviation values in Fig. 6. It can be also observed that the increase of sonication duration from 0.5 to 5 h resulted in an increase of surface roughness of *M*2–*M*4 membranes. It could be postulated that application of longer sonication time led to formation of smaller agglomerates, but they were moved closer to the membrane surface, which caused the higher hills to be formed on it. In the case of *M*5–*M*7 the increase of the sonication amplitude from 40% to 60% resulted in a

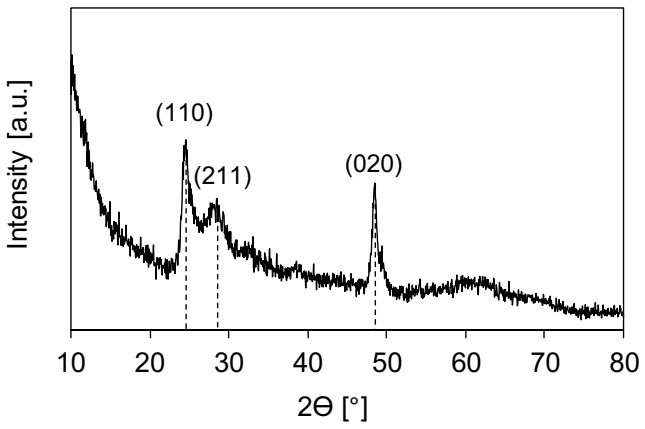

Fig. 1. XRD pattern of the prepared titanate nanotubes.

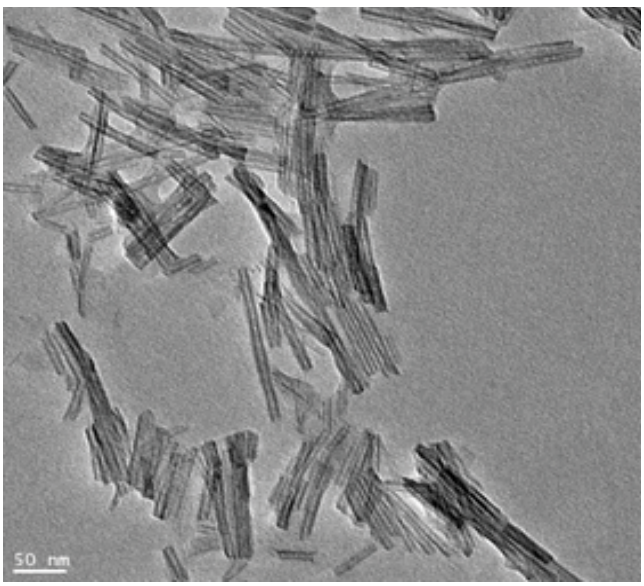

Fig. 2. TEM image of the prepared TNTs.

slight increase of R_a, while further rise to 80% did not led to any significant changes of the surface roughness. Although in general the increase of the amplitude of horn vibration allows to enhance the cavitation intensity in the sample, the results summarized in Fig. 6 suggest that in case of the examined membranes the amplitude higher that 60% does not further contribute to a better dispersion of TNTs on the membranes surface. On a basis of the AFM analysis, it can be concluded that the TNTs dispersion procedure influenced the topography and roughness of the surface of the mixed-matrix membranes due to the different size and distribution of the nanofiller.

The analysis of zeta potential of membranes revealed that the isoelectric point of the unmodified *M*1 was slightly

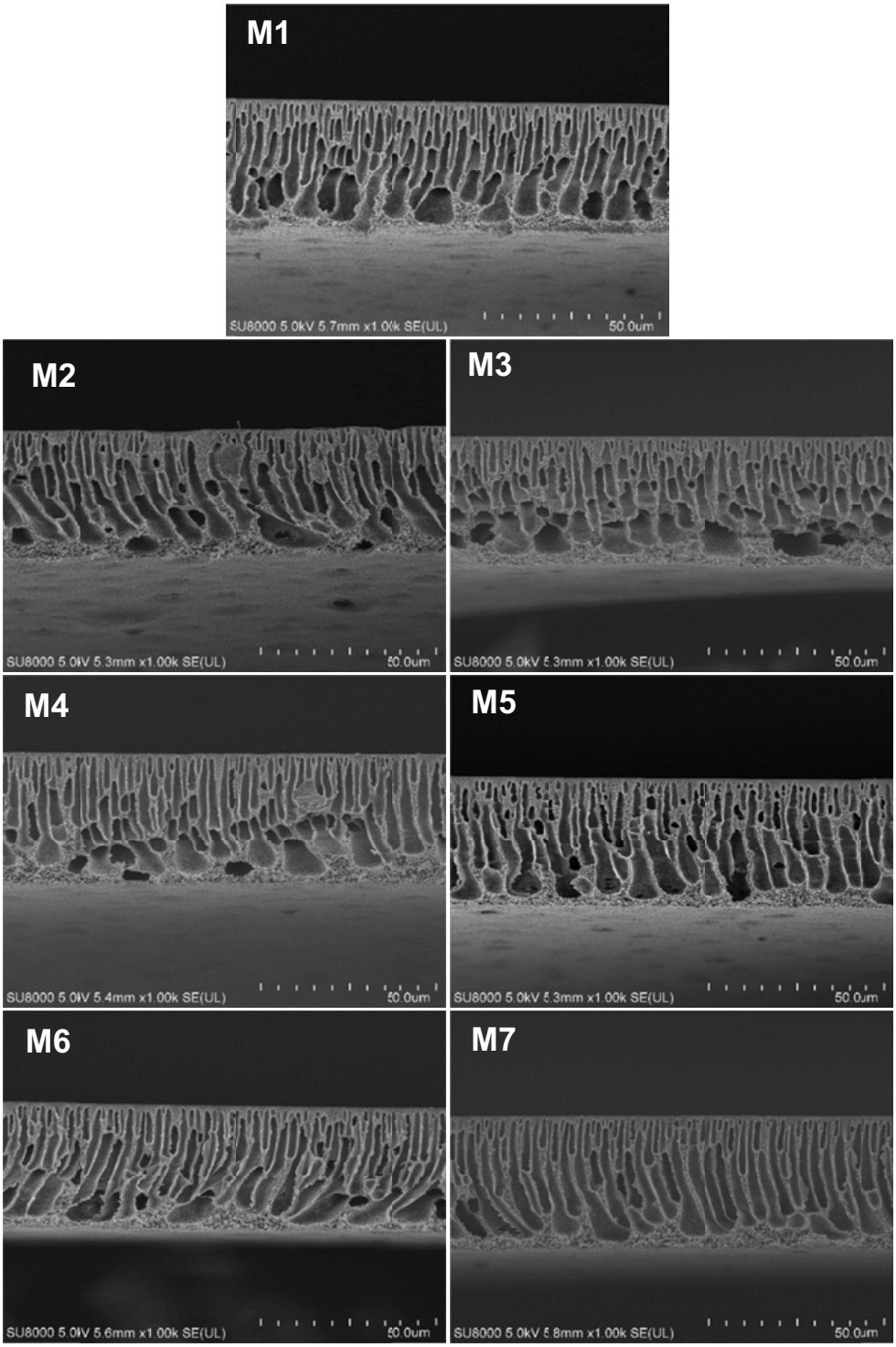

Fig. 3. SEM images of cross-sections of the unmodified *M*1 and TNTs-modified membranes.

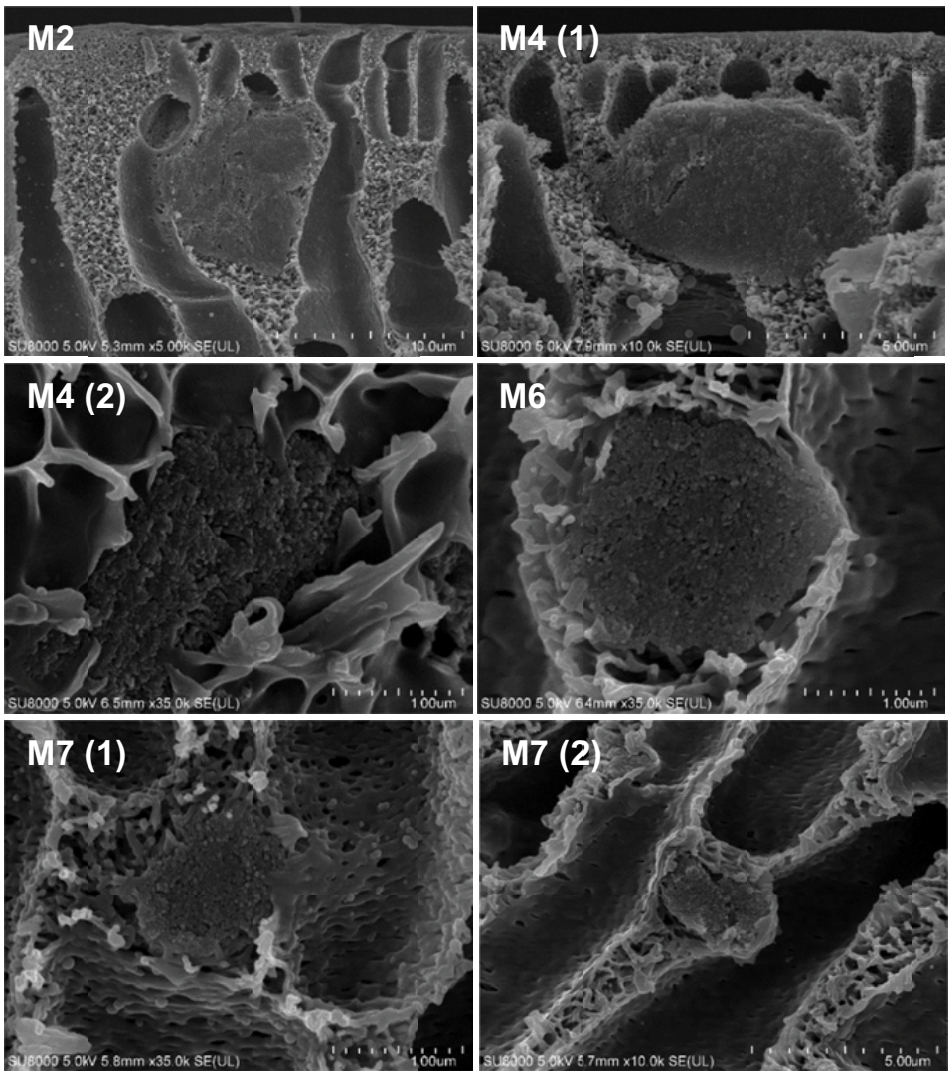

Fig. 4. SEM images of TNTs agglomerates in the cross-sections of the modified membranes.

higher (2.7) than that observed for the TNTs-modified samples (2.3–2.4). These results indicate that incorporation of TNTs in PES membrane matrix influenced its surface properties. Nonetheless, no effect of the TNTs dispersion procedure on the isoelectric point of the composite membranes was found. That can be attributed to the same loading (1 wt.% vs. PES) of the nanofiller in all the membranes.

3.3. Water permeability of membranes

Fig. 7 presents PWF values determined for various membranes.

In general, the fluxes measured for the membranes obtained according to the procedure No. 1 were lower compared to those in case of the procedure No. 2. This phenomenon can be attributed to a poorer dispersion of TNTs in the membrane structure associated with milder conditions during sonication using ultrasonic bath compared to ultrasonic probe. Furthermore, the lowest permeate flux amongst the membranes modified according to the procedure No. 1 was found in the case of *M*2, for which the time of sonication was the shortest (0.5 h). Extension of the sonication period up to 5 h resulted in a slight improvement of water permeability. Nonetheless, the highest PWF values were measured for *M*6 and *M*7 membranes, in case of which the TNTs were dispersed using an ultrasonic probe operated at high (60% and 80%, respectively) amplitude.

The enhancement of water permeability in case of the membranes modified with TNTs is attributed to the easier water penetration due to the hydrophilic character of TNTs [25,30], as well as to the open-ended nanotubular morphology which results in the presence of the additional pores in the membrane matrix [34]. Nonetheless, the positive effect can be reduced at higher concentrations of the TNTs due to their agglomeration [30]. Thus, the dispersion of the nanotubes is a crucial factor affecting the membranes performance [40]. The data summarized in Fig. 7 revealed that the conditions of TNTs dispersion in the solvent affected the membranes permeability. Therefore, it was concluded that the careful selection of the casting dope preparation

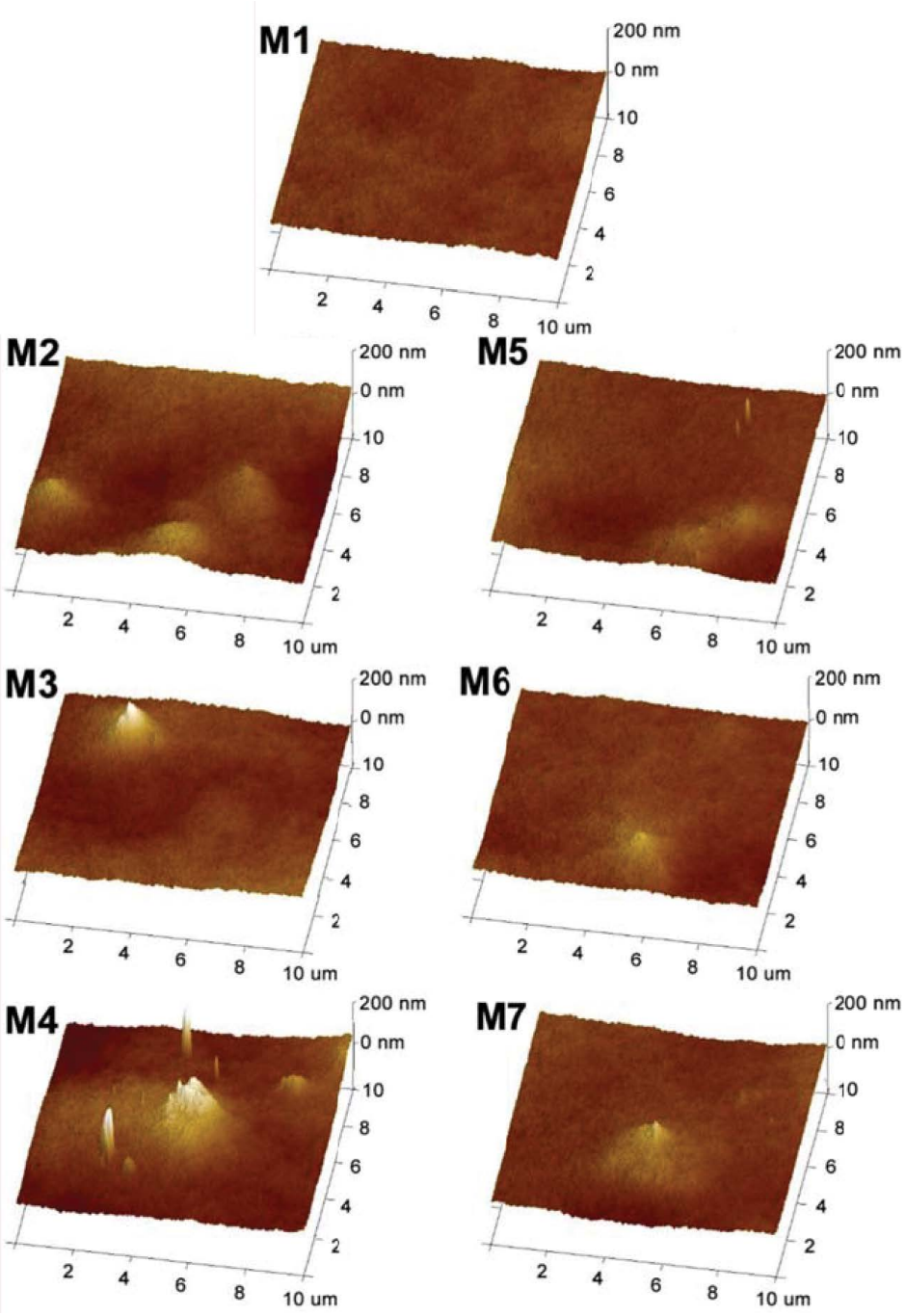

Fig. 5. Three-dimensional AFM images of the surfaces of the studied membranes.

conditions could lead to the improved dispersion of the TNTs in the polymer matrix and formation of smaller agglomerates in the membrane structure, which contributes to the increase of the permeability.

3.4. Separation characteristics of membranes

Fig. 8 summarizes rejection characteristics of the unmodified *M*1 membrane and the mixed-matrix membranes prepared under various conditions. As can be found, the dispersion of TNTs in the PES membrane had a significant influence on its separation properties. The least effect of the presence of the nanofiller was observed for *M*2, in case of which the separation characteristics was similar to that of the unmodified membrane. Elongation of the sonication time contributed to a slight improvement of the separation properties of the membranes obtained according to the procedure No. 1. For example, the rejection of PEG with MW of 35 kDa increased from 46% for *M*2 to 56% for *M*3 and *M*4, while the rejection of the 110 kDa dextran changed

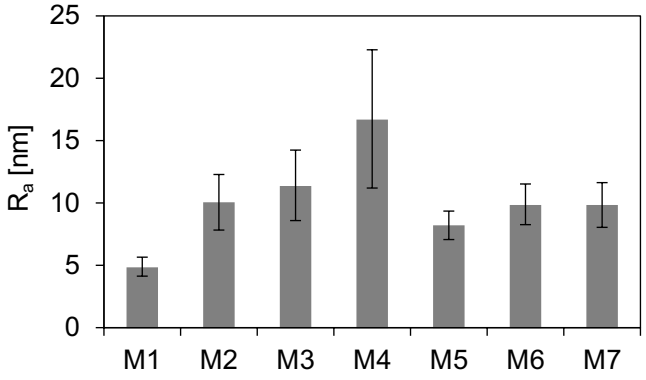

Fig. 6. Mean surface roughness (R_a) of the neat (*M*1) and mixed-matrix (*M*2–*M*7) membranes.

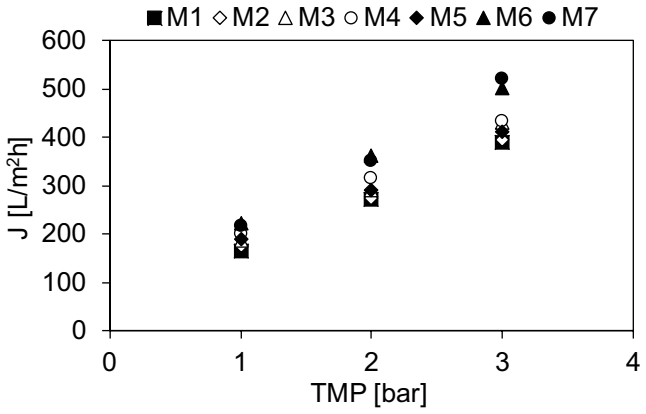

Fig. 7. Influence of the procedure of TNTs dispersion in DMF on pure water flux through the membranes. Transmembrane pressure: 1–3 bar.

from 68% for *M*2 to 73 for *M*3 and 81% for *M*4. For comparison, the corresponding values of *R* calculated for the unmodified *M*1 were equal to 48% and 72%, respectively. These data show that poor dispersion of TNTs may lead to formation in the skin layer of some pores with larger diameters than those in the unmodified membrane. That can contribute to a slight deterioration of separation properties, which was especially visible in case of *M*2.

The change of the modification method to the procedure No. 2 resulted in a significant improvement of the separation characteristics of the composite membranes. Moreover, the influence of the sonication amplitude on the rejection of the model organic compounds was also observed. For example, the rejection of 20 kDa PEG changed from 43% for *M*5 to 71% for *M*7, while in case of 35 kDa PEG it increased from 67% for *M*5 to 87% for *M*7. The differences in case of dextrans, characterized by higher MW, were not so pronounced. The value of *R* calculated for 70 kDa dextran ranged from 84% to 86%, while that in case of 110 kDa dextran was 88%–91%, for *M*5–*M*7, respectively.

The obtained results revealed that some relation between the dispersion of the TNTs and the separation properties of the obtained membranes exists. In general, the membranes containing large and poorly dispersed TNTs agglomerates

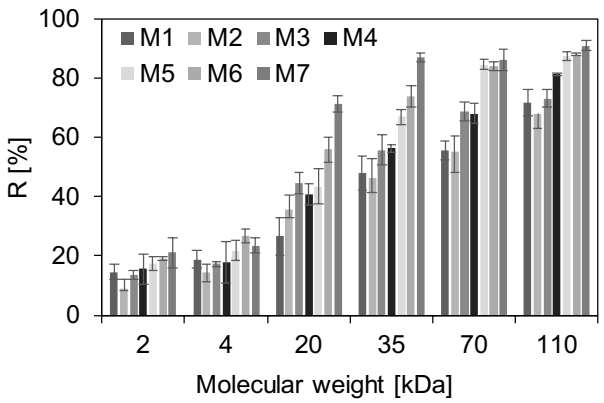

Fig. 8. Rejection coefficient *R* of the obtained membranes. The molecular weight of 2, 4, 20, and 35 kDa corresponds to various PEGs, while 70 and 110 kDa refers to dextrans.

exhibited also lower rejection of the model compounds. On the opposite, the membranes containing smaller TNTs agglomerates were characterized by the best separation properties. These data confirm that application of the direct sonication method is more advantageous not only in terms of water permeability but also with reference to the separation properties of the mixed-matrix membranes.

3.5. Antibacterial properties of membranes

The antimicrobial properties of the unmodified (*M*1) and composite (*M*2–*M*7) membranes were estimated with application of *E. coli* as model bacteria. The results are summarized in Fig. 9. It can be observed that the unmodified (*M*1) membrane did not present any significant antibacterial abilities (log reduction value reached ca. 0.06). In contrast, the presence of TNTs in the structure of the membranes contributed noticeably to a decrease of the number of bacteria. The best antimicrobial performance exhibited the *M*4 membrane. The log reduction amounted in that case ca. 0.3, which corresponded to almost 50% inhibition of bacterial growth. The antibacterial performance of the membranes prepared according to the procedure No. 2 was visibly lower compared to those fabricated with application of the procedure No. 1. The log reduction in case of *M*5–*M*7 was in the range of ca. 0.1–0.18, being similar for the samples obtained under 60% and 80% amplitude.

Considering that the concentration of TNTs was in case of all the samples maintained on the unchanged level (i.e., 1 wt.% vs. PES), the differences in the results reported in Fig. 9 could be attributed to the dispersion of the nanofiller on the membrane surface. A correlation between the roughness and antibacterial activity of the obtained membranes was found. The results presented in Fig. 10 show that there is a linear relationship (R^2 = 0.94) between the antibacterial activity of the mixed-matrix membranes and their roughness. The *M*2, *M*6, and *M*7 have very similar roughness of the surface and the antibacterial activity of these membranes was also on a quite same level. The best antimicrobial properties were noted for the *M*4 membrane with the highest R_a values.

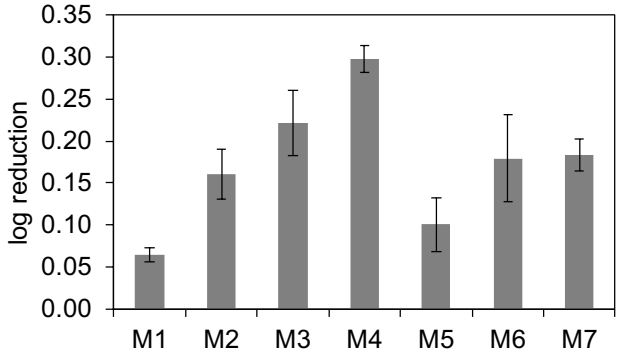

Fig. 9. Influence of the preparation procedure of the membranes on *Escherichia coli* survival.

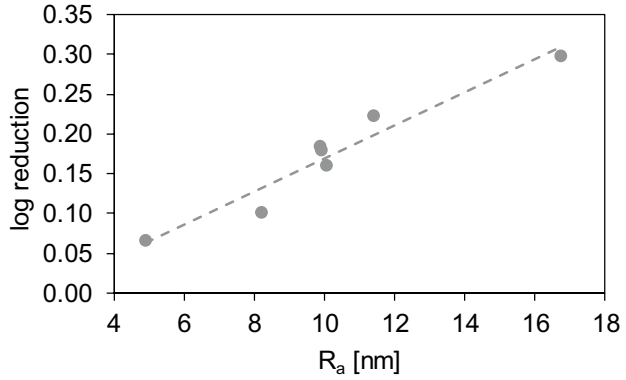

Fig. 10. Correlation between antibacterial activity and roughness of the *M1*–*M7* membranes.

To further evaluate the effect of TNTs on *E. coli* removal, the SEM analysis of the bacteria cells on the surface of the membranes was performed. Figs. 11a and b show the undamaged and damaged bacteria found on the unmodified membrane. The presence of both forms of cells results from the typical bacteria life cycle. Moreover, the destruction of bacteria cells (Fig. 11b) could be attributed to the mixing of the suspension using a magnetic stirrer. Figs. 11c and d show SEM images of bacteria present on the TNTs-modified membrane. In this case also two types of bacteria morphology were found: undamaged (Fig. 11c) and damaged (Fig. 11d) cells. It was noted, however, that much more *E. coli* bacteria had fragmented and destroyed cell envelopes in case of the TNTs-modified membrane compared to the unmodified one. The bacteria cells on the TNTs-modified membrane (Fig. 11d) were noticeably smaller (this may indicate leakage of the cell contents) and even totally burst. Considering that the experimental conditions remained the same for the unmodified and modified membranes, it can be postulated that the observed changes in the *E. coli* morphology are the result of the mechanical damage of the bacteria cells by the needle-like TNTs structures (Fig. 5). Cylindrical shape and high aspect ratio of the TNTs can cause penetration and damage of the outer layer of the microbial cells, provoking the release of the intracellular content. It should be noted that this type of bacterial killing mechanism has already been observed in many studies describing membranes modified with carbon nanotubes (CNTs) [41–43].

The antibacterial mechanisms of TNTs are widely discussed by Li et al. [44] in their recent review on orthopedic implants. Some proposed pathways can be also adopted to explain the antibacterial action of the TNTs-modified membranes. In general, the antibacterial mechanism is

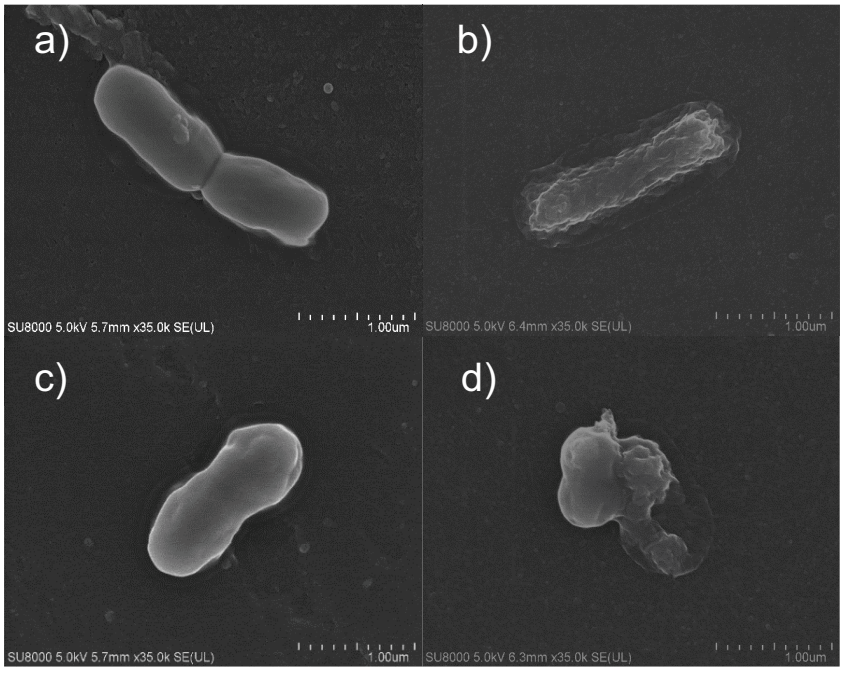

Fig. 11. SEM images of: undamaged (a) and damaged (b) bacteria present on neat PES membrane; and undamaged (c) and damaged (d) bacteria present on TNTs-modified membrane surface.

referred to the surface roughness, charge repulsion, and cell membrane stretching. The roughness affects hydrophilicity and it was concluded that in the presence of TNTs the surface becomes more hydrophilic, which hinders the adhesion of the hydrophobic bacteria. Moreover, in the nanoscale (10–100 nm) the bacteria adhesion decreases with the increase of roughness, while in the case of microscale the adhesion increases with the roughness, which phenomena can be explained by the attach point theory [44]. The charge repulsion between the negatively charged TNTs present on the membrane surface and the negatively charged bacteria also counteracts the initial adhesion. The discussed above pathways explain the decreased deposition of bacteria on TNTs-containing surfaces. Nonetheless, the most important mechanism in case of the inhibition of bacterial growth in the presence of the mixed-matrix membranes seems to be the cell membrane stretching. This phenomenon is strictly related to the surface topography of the TNTs-modified membranes. The stretching forces between TNTs and bacteria can accelerate bacteria inactivation [44]. When bacteria are in contact with TNTs, the protruding TNTs pillars may cause a deformation of bacterial cell membrane and if the stretching exceeds a critical value the cell membrane eventually ruptures leading to bacteria death [45]. In case of the stretching mechanism the surface roughness and the density and shape of the pillars present on the surface were found to be important. The high roughness and the pillars inhomogeneity were reported to be the factors enhancing the stretching degree and contributing to the improvement in the bactericidal efficiency [45]. The importance of surface roughness has been also confirmed on a basis of the data presented in Fig. 10.

Based on the above results, it was concluded that the inhibition of bacterial growth took place by a mechanical disruption of the cell walls. It was found that the surface roughness of the membranes played a key role in their antibacterial ability. The best antibacterial properties were noted for the membrane exhibiting the highest surface roughness (*M*4). Except from the roughness also the size and shape of agglomerates were found to be important factors affecting the antibacterial properties. On the surface of the *M*4 membrane some needle-like TNTs agglomerates with relatively small diameters were observed, which could possibly contribute to the improvement of the antibacterial ability of the membrane as well.

4. Conclusions

The present study revealed that the procedure of preparation of casting solution for fabrication of TNTs-modified PES membranes via wet phase inversion technique has essential influence on their physicochemical, transport, separation, and antimicrobial properties. In order to limit the agglomeration of TNTs in the polymer matrix, several procedures of NPs dispersion in DMF solvent were devised using two types of sonication techniques (direct vs. indirect). It was proved that both the type of sonication as well as the parameters of its realization affected the membrane morphology and performance.

In general, the incorporation of TNTs into the PES membrane improved its transport and separation properties, although the observed effect was more pronounced in case of the membranes prepared according to the procedure No. 2 (i.e., using direct sonication) compared to the procedure No. 1. The highest improvement of water permeability was observed for the *M*6 and *M*7 membranes fabricated with application of the ultrasonic probe operated at amplitude of 60% and 80%, respectively. The rejection of PEGs and dextrans with various MW was the highest in case of *M*7 membrane. The *R*-value calculated for 35 kDa PEG was 87% in case of *M*7 which was almost two times higher than observed for the unmodified *M*1 (48%).

Moreover, significant influence of the casting dope preparation procedure on the antibacterial properties of the membranes evaluated on a basis of *E. coli* inactivation was demonstrated. In general, the membranes fabricated according to the procedure No. 1 exhibited higher antibacterial activity than those prepared using the procedure No. 2. The key parameters affecting the antibacterial performance of the membranes were found to be the surface roughness as well as the shape and size of TNTs agglomerates. A linear correlation between R_a and the log reduction values was confirmed. The best antimicrobial performance revealed the *M*4 membrane with the highest surface roughness. The inhibition of *E. coli* growth in the presence of *M*4 was about five times higher compared to the unmodified *M*1 membrane (log reduction: 0.3 vs. 0.06, respectively).

Moreover, it was noticed that the effect of the dispersion procedure on the water permeability of the membranes and their antibacterial properties was opposite. In other words, the formation of smaller TNTs agglomerates in case of the direct sonication was beneficial in terms of permeability but unfavorable when the antibacterial properties of the membranes are considered. Similarly, formation of larger agglomerates in case of the indirect sonication resulted in a more rough membrane surface which improved its antimicrobial properties, but at the same time, the permeability has deteriorated. These results show that it is necessary to find a balance between permeability and antimicrobial properties of the membranes by a careful selection of conditions of casting dope preparation.

Acknowledgments

This work was supported by the National Science Centre, Poland under Project No. 2016/21/B/ST8/00317.

The authors would like to thank Solvay Polska Sp. z o.o. for providing polyethersulfone samples.

Symbols and abbreviations

A	—	Amplitude
AFM	—	Atomic force microscopy
AOC	—	Assimilable organic carbon
B	—	Amount of bacteria (CFU/mL) in a blank sample
C_f	—	Concentration of model compounds in feed
CFU	—	colony forming unit
CNTs	—	Carbon nanotubes
C_p	—	Concentration of model compounds in permeate
DMF	—	*N*,*N*-dimethylformamide

HNTs — Halloysite nanotubes
MW — Molecular weight
n — Number of bacteria colonies visible on a Petri dish
NPs — Nanoparticles
PCA — Plate count agar
PEG — Polyethylene glycol
PES — Polyethersulfone
PVA — Poly(vinyl alcohol)
PVDF — Polyvinylidene fluoride
PWF — Pure water flux
R — Rejection coefficient
R_a — Mean roughness
S — Amount of bacteria (CFU/mL) in the presence of a membrane
TEM — Transmission electron microscopy
TMP — Transmembrane pressure
TNTs — Titania nanotubes, titanate nanotubes
UHR FE-SEM — Ultra-high resolution field emission scanning electron microscopy
v — Volume of bacteria suspension placed on the Petri dish
VCF — Feed cross-flow velocity
x — Dilution factor
XRD — X-ray diffraction
ZVI — Zerovalent iron

References

[1] G. Amy, N. Ghaffour, Z. Li, L. Francis, R. Valladares Linares, T. Missimer, S. Lattemann, Membrane-based seawater desalination: present and future prospects, Desalination, 401 (2017) 16–21.
[2] A. Figoli, A. Criscuoli, Sustainable Membrane Technology for Water and Wastewater Treatment, 1st ed., Springer, Singapore, 2017.
[3] H.K. Shon, S. Phuntsho, D.S. Chaudhary, S. Vigneswaran, J. Cho, Nanofiltration for water and wastewater treatment – a mini review, Drinking Water Eng. Sci., 6 (2013) 47–53.
[4] A.W. Mohammad, C.Y. Ng, Y.P. Lim, G.H. Ng, Ultrafiltration in food processing industry: review on application, membrane fouling, and fouling control, Food Bioprocess Technol., 5 (2012) 1143–1156.
[5] P. Kumar, N. Sharma, R. Ranjan, S. Kumar, Z.F. Bhat, D.K. Jeong, Perspective of membrane technology in dairy: a review, Asian-Australas. J. Anim. Sci., 26 (2013) 1347–1358.
[6] D. Chen, K.K. Sirkar, C. Jin, D. Singh, R. Pfeffer, Membrane-based technologies in the pharmaceutical industry and continuous production of polymer-coated crystals/particles, Curr. Pharm. Des., 23 (2017) 242–249.
[7] A. Saxena, B.P. Tripathi, M. Kumar, V.K. Shahi, Membrane-based techniques for the separation and purification of proteins: an overview, Adv. Colloid Interface Sci., 145 (2009) 1–22.
[8] L.E. Applegate, C.W. Erkenbrecher, Monitoring and control of biological activity in Permasep® seawater RO plants, Desalination, 65 (1987) 331–359.
[9] D. Kim, S. Jung, J. Sohn, H. Kim, S. Lee, Biocide application for controlling biofouling of SWRO membranes – an overview, Desalination, 238 (2009) 43–52.
[10] M. Polanska, K. Huysman, C. van Keer, Investigation of assimilable organic carbon (AOC) in flemish drinking water, Water Res., 39 (2005) 2259–2266.
[11] F. Hammes, S. Meylan, E. Salhi, O. Koster, T. Egli, U. von Gunten, Formation of assimilable organic carbon (AOC) and specific natural organic matter (NOM) fraction during ozonation of phytoplankton, Water Res., 41 (2007) 1447–1454.
[12] S.-H. Zhi, R. Deng, J. Xu, L.-S. Wan, Z.-K. Xu, Composite membranes from polyacrylonitrile with poly(*N*,*N*-dimethylaminoethyl methacrylate)-grafted silica nanoparticles as additives, React. Funct. Polym., 86 (2015) 184–190.
[13] A. Qin, X. Li, X. Zhao, D. Liu, C. He, Engineering a highly hydrophilic PVDF membrane via binding TiO_2 nanoparticles and a PVA layer onto a membrane surface, ACS Appl. Mater. Interfaces, 7 (2015) 8427–8436.
[14] H.L. Richards, P.G.L. Baker, E. Iwuoha, Metal nanoparticle modified polysulfone membranes for use in wastewater treatment: a critical review, J. Surf. Eng. Mater. Adv. Technol., 2 (2012) 183–193.
[15] B. Ma, W. Yu, W.A. Jefferson, H. Liu, J. Qu, Modification of ultrafiltration membrane with nanoscale zerovalent iron layers for humic acid fouling reduction, Water Res., 71 (2015) 140–149.
[16] J. Lee, Y. Ye, A.J. Ward, C. Zhou, V. Chen, A.I. Minett, S. Lee, Z. Liu, S.-R. Chae, J. Shi, High flux and high selectivity carbon nanotube composite membranes for natural organic matter removal, Sep. Purif. Technol., 163 (2016) 109–119.
[17] Z. Wang, H. Wang, J. Liu, Y. Zhang, Preparation and antifouling property of polyethersulfone ultrafiltration hybrid membrane containing halloysite nanotubes grafted with MPC via RATRP method, Desalination, 344 (2014) 313–320.
[18] I. Sawada, R. Fachrul, T. Ito, Y. Ohmukai, T. Maruyama, H. Matsuyama, Development of a hydrophilic polymer membrane containing silver nanoparticles with both organic antifouling and antibacterial properties, J. Membr. Sci., 387–388 (2012) 1–6.
[19] Z. Wang, X. Chen, K. Li, S. Bi, C. Wu, L. Chen, Preparation and catalytic property of PVDF composite membrane with polymeric spheres decorated by Pd nanoparticles in membrane pores, J. Membr. Sci., 496 (2015) 95–107.
[20] A. Razmjou, J. Mansouri, V. Chen, The effects of mechanical and chemical modification of TiO_2 nanoparticles on the surface chemistry, structure and fouling performance of PES ultrafiltration membranes, J. Membr. Sci., 378 (2011) 73–84.
[21] V. Kochkodan, N. Hilal, V. Goncharuk, L. Al-Khatib, T. Levadna, Effect of the surface modification of polymer membranes on their microbiological fouling, Colloid J., 68 (2006) 267–273.
[22] W. Liu, J. Ni, X. Yin, Synergy of photocatalysis and adsorption for simultaneous removal of Cr(VI) and Cr(III) with TiO_2 and titanate nanotubes, Water Res., 53 (2014) 12–25.
[23] Q. Chen, L. Peng, Structure and applications of titanate and related nanostructures, Int. J. Nanotechnol., 4 (2007) 44–65.
[24] H. Abdallah, A.F. Moustafa, A.A. AlAnezi, H.E.M. El-Sayed, Performance of a newly developed titanium oxide nanotubes/polyethersulfone blend membrane for water desalination using vacuum membrane distillation, Desalination, 346 (2014) 30–36.
[25] A. Sumisha, G. Arthanareeswaran, A.F. Ismail, D.P. Kumar, M.V. Shankar, Functionalized titanate nanotube–polyetherimide nanocomposite membrane for improved salt rejection under low pressure nanofiltration, RSC Adv., 5 (2015) 39464–39473.
[26] M. Padaki, D. Emadzadeh, T. Masturra, A.F. Ismail, Antifouling properties of novel PSf and TNT composite membrane and study of effect of the flow direction on membrane washing, Desalination, 362 (2015) 141–150.
[27] M. Shaban, H. Abdallah, L. Said, H.S. Hamdy, A.A. Khalek, Titanium dioxide nanotubes embedded mixed matrix PES membranes characterization and membrane performance, Chem. Eng. Res. Des., 95 (2014) 307–316.
[28] R. Kumar, H. Al-Jabli, S. Al-Haddad, M. Al-Rughaib, J. Samuel, Modified titanate nanotubes incorporated polyamide layer for the fabrication of fouling control thin-film nanocomposite forward osmosis membranes, Desal. Water Treat., 69 (2017) 56–64.
[29] I.H. Alsohaimi, M. Kumar, M.S. Algamdi, M.A. Khan, K. Nolan, J. Lawler, Antifouling hybrid ultrafiltration membranes with high selectivity fabricated from polysulfone and sulfonic acid functionalized TiO_2 nanotubes, Chem. Eng. J., 316 (2017) 573–583.
[30] M.N. Subramaniam, P.S. Goh, W.J. Lau, B.C. Ng, A.F. Ismail, Hydrophilic hollow fiber PVDF ultrafiltration membrane incorporated with titanate nanotubes for decolourization

of aerobically-treated palm oil mill effluent, Chem. Eng. J., 316 (2017) 101–110.
[31] M.N. Subramaniam, P.S. Goh, W.J. Lau, B.C. Ng, A.F. Ismail, AT-POME colour removal through photocatalytic submerged filtration using antifouling PVDF-TNT nanocomposite membrane, Sep. Purif. Technol., 191 (2018) 266–275.
[32] Z. Raeisi, A. Moheb, M. Sadeghi, A. Abdolmaleki, M. Alibouri, Titanate nanotubes–incorporated poly(vinyl alcohol) mixed matrix membranes for pervaporation separation of water-isopropanol mixtures, Chem. Eng. Res. Des., 145 (2019) 99–111.
[33] S. Mozia, M. Jose, P. Sienkiewicz, K. Szymański, D. Darowna, M. Zgrzebnicki, A. Markowska-Szczupak, Polyethersulfone ultrafiltration membranes modified with hybrid Ag/titanate nanotubes: physicochemical characteristics, antimicrobial properties, and fouling resistance, Desal. Water Treat., 128 (2018) 106–118.
[34] K. Szymański, D. Darowna, P. Sienkiewicz, M. Jose, K. Szymańska, M. Zgrzebnicki, S. Mozia, Novel polyethersulfone ultrafiltration membranes modified with Cu/titanate nanotubes, J. Water Process Eng., 33 (2020) 101098, doi: 10.1016/j.jwpe.2019.101098.
[35] T. Kasuga, M. Hiramatsu, A. Hoson, T. Sekino, K. Niihara, Formation of titanium oxide nanotube, Langmuir, 14 (1998) 3160–3163.
[36] S. Preda, M. Rutar, P. Umek, M. Zaharescu, A study of thermal properties of sodium titanate nanotubes synthesized by microwave-assisted hydrothermal method, Mater. Res. Bull., 71 (2015) 98–105.
[37] G.R. Lima, W.F. Monteiro, R. Ligabue, R.M.C. Santana, Titanate nanotubes as new nanostructured catalyst for depolymerization of PET by glycolysis, Mater. Res., 20 (2017) 588–595.
[38] M. Jose, P. Sienkiewicz, K. Szymańska, D. Darowna, D. Moszyński, Z. Lendzion-Bieluń, K. Szymański, S. Mozia, Influence of preparation procedure on physicochemical and antibacterial properties of titanate nanotubes modified with silver, Nanomaterials, 9 (2019) 795, doi: 10.3390/nano9050795.
[39] M. Güney, A. Elik, Comparison of probe with bath ultrasonic leaching procedures for preparation to heavy metal analysis of bio-collectors prior to atomic absorption spectrometry, Commun. Soil Sci. Plant Anal., 48 (2017) 1741–1752.
[40] Z.C. Ng, C.Y. Chong, W.J. Lau, M. Karaman, A.F. Ismail, Boron removal and antifouling properties of thin-film nanocomposite membrane incorporating PECVD-modified titanate nanotubes, J. Chem. Technol. Biotechnol., 94 (2019) 2772–2782.
[41] M. Majunder, N. Chora, R. Andrews, B.J. Hinds, Nanoscale hydrodynamics: enhanced flow in carbon nanotubes, Nature, 438 (2005) 44, doi: 10.1038/43844a.
[42] D. Mattia, H. Leese, K.P. Lee, Carbon nanotube membranes: from flow enhancement to permeability, J. Membr. Sci., 475 (2015) 266–272.
[43] X. Qin, Q. Yuan, Y. Zhao, S. Xie, Z. Lin, Measurement of rate of water translocation through carbon nanotubes, Nano Lett., 11 (2011) 2173–2177.
[44] Y. Li, Y. Yang, R. Li, X. Tang, D. Guo, Y. Qing, Y. Qin, Enhanced antibacterial properties of orthopedic implants by titanium nanotube surface modification: a review of current techniques, Int. J. Nanomed., 14 (2019) 7217–7236.
[45] S. Wu, F. Zuber, K. Maniura-Weber, J. Brugger, Q. Ren, Nanostructured surface topographies have an effect on bactericidal activity, J. Nanobiotechnology, 16 (2018) 20, doi: 10.1186/s12951-018-0347-0.